JOURNAL OF AGRICULTURAL AND FOOD CHEMISTRY

pubs.acs.org/JAFC Article

BLA1 Affects Leaf Angles by Altering Brassinosteroid Biosynthesis in Rice (*Oryza sativa* L.)

Yanli Zhang, Guojun Dong, Ying Zhang, Yaohuang Jiang, Fei Chen, Banpu Ruan, Limin Wu,* and Yanchun Yu*

Cite This: *J. Agric. Food Chem.* 2024, 72, 19629−19643 Read Online

ACCESS | Metrics & More | Article Recommendations | Supporting Information

ABSTRACT: Brassinosteroids (BRs) are crucial plant hormones influencing diverse developmental processes in rice. While several enzymes in BR biosynthesis have been identified, their regulatory mechanisms remain largely unknown. This study highlights a novel regulatory pathway wherein the CHD3 chromatin remodeler, *BLA1*, epigenetically modulates the expression of key BR biosynthesis genes, *BRD1* and *D2*. Phenotypic analysis of *bla1* mutants revealed significant alterations, such as increased leaf angles and longer mesocotyls, which were alleviated by BR synthesis inhibitors. Moreover, the *bla1* mutants showed elevated BR levels that correlated with the significant upregulation of the expression levels of *BRD1* and *D2*, particularly at the lamina joint sites. Mechanistically, the yeast one-hybrid and chromatin immunoprecipitation assays revealed specific binding of BLA1 to the promoter regions of *BRD1* and *D2*, accompanied by a marked enrichment of the transcriptionally active histone modification, H3K4me3, on these loci in the *bla1* mutant. Functional assessments of the *brd1* and *d2* mutants confirmed their reduced sensitivity to BR, further underscoring their critical regulatory roles in BR-mediated developmental processes. Our findings uncovered an epigenetic mechanism that governs BR biosynthesis and orchestrates the expression of *BRD1* and *D2* to modulate BR levels and influence rice growth and development.

KEYWORDS: *leaf angle, mesocotyl elongation, chromatin remodeler, Brassinosteroid biosynthesis, histone modification, phytohormone, rice (Oryza sativa L.)*

Downloaded via HANGZHOU NORMAL UNIV on October 23, 2024 at 10:17:06 (UTC).
See https://pubs.acs.org/sharingguidelines for options on how to legitimately share published articles.

INTRODUCTION

Brassinosteroids (BRs), a class of plant steroid hormones, play pivotal roles in regulating various physiological processes, such as cell expansion and division, vascular differentiation, seed germination, photomorphogenesis, flowering, senescence, and responses to environmental stresses.[1] In rice (*Oryza sativa* L.), BRs exert a specific influence on leaf angle modulation, primarily by facilitating cell expansion on the adaxial side while modulating cell division on the abaxial side.[2] This precise regulation is essential to optimize canopy photosynthesis, thereby enhancing light penetration to lower leaves and ultimately increasing crop yields.[3] Understanding the genetic mechanisms governing BR biosynthesis in rice holds significant promise for agricultural advancement. By elucidating the genes involved in BR biosynthesis and their regulatory pathways, researchers can develop targeted strategies to effectively manipulate BR levels. Such endeavors not only enhance our comprehension of fundamental plant biology but also offer practical solutions for optimizing crop productivity and resilience in response to fluctuating environmental conditions.

Over the years, both forward and reverse genetics approaches have been instrumental in dissecting the biosynthesis routes of BRs. Currently, three distinct pathways leading to the production of C27-, C28-, and C29-type BRs have been identified.[4] The synthesis of cycloartenol, a plant-specific C30 sterol and a precursor to BRs, initiates from squalene through two pathways: the nonmevalonate and mevalonate pathways.[5] Enzymes, such as squalene epoxidase (SQE) and cycloartenol synthase (CAS), play crucial roles in the conversion of squalene to cycloartenol.[6] The synthetic pathway branches into three distinct routes: the cholesterol branch, the campesterol branch, and the sitosterol branches.[4] Within these branches, a multitude of genes, including *SMO2*, *DWF7*, *DWF5*, *DWF1*, *SMT2*, *SSR2*, *SMO3*, *SMO4*, and *DET2*, orchestrate various enzymatic reactions.[7] Among the BRs, C28-type BRs that are synthesized from campesterol are notably abundant in plants, while C27 and C29 BRs are derived from cholesterol and sitosterol, respectively.[8] The biosynthesis pathway of C28 BRs has been extensively studied, primarily in *Arabidopsis thaliana*.[9] Campesterol undergoes oxidation pathways to yield campestanol (CN) and campestanol (CS).[8] Additionally, campesterol can be converted into 6-deoxocathasterone via an early C22 oxidation pathway or 3-dehydro-6-deoxoteasterone via a C23 hydroxylation pathway, leading to the synthesis of CS.[9] Enzymes such as DWF4, CYP724A1, CYP90C1, CTP90D1, CTP90A1, DET2, and CYP85A1/2 are instrumental in these processes.[10] However, compared with model plant species, our understanding of BR biosynthesis pathways in rice, a staple food crop, remains limited. While a few genes related to BR biosynthesis have been identified, including OsCYP51G3,[11] BRD2,[12] OsDWF4,[13] D2,[14] CPD1, CPD2,[15] D11,[16] and

Received: May 17, 2024
Revised: August 12, 2024
Accepted: August 26, 2024
Published: August 29, 2024

ACS Publications © 2024 American Chemical Society

BRD1,[17] the overall pathway in rice requires further elucidation. D2 is a critical enzyme in the BR synthesis pathway, operating at the C3 dehydrogenation steps. It is responsible for converting teasterone (TE) to 3-dehydroteaserone (3DT) and 6-deoxoTE to 6-deoxo3DT, acting upstream of BRD1.[7] Additional research efforts are warranted to uncover novel genes and regulatory mechanisms governing BR biosynthesis in rice, and this could have significant implications for crop improvement and agricultural sustainability.

To achieve optimal growth and development, plants must carefully regulate internal levels of BR. These steroid hormones are curtailed, but their excess can be detrimental.[18] In rice, the balance of BRs is maintained through complex and diverse mechanisms. For instance, other hormones influence BR levels; the gene OsGSR1, a member of the GA-stimulated transcript gene family, is activated by GA and interacts with DIM/DWF1 to modulate BR levels.[19] Additionally, hormonal treatments, such as methyl jasmonate (MeJA), suppress the expression of genes related to BR biosynthesis, thus reducing endogenous BR levels.[20] Abscisic acid also mitigates BR effects on the bending of leaf joints by targeting specific BR biosynthesis and signaling genes.[21] Moreover, environmental factors such as light play a significant role in BR biosynthesis. Blue light increases CS levels in aerial tissues, while far-red light adjusts them in roots.[22] Epigenetic factors are also critical, and modifications such as the methylation of histone H3K36 by the rice enzyme SDG725 influence BR-related gene expression.[23] RAV6 epigenetic modification is essential for BR homeostasis maintenance,[24] highlighting the importance of epigenetic regulation in BR biosynthesis. However, the potential effect of other histone modifications, such as H3K4 methylation, on BR biosynthesis remains an intriguing question. Furthermore, melatonin and O-linked N-acetylglucosamine transferase repress BR biosynthesis through an unknown mechanism.[25]

Proteins that bind to chromosome helicase DNA (CHD) play crucial roles in gene regulation across various stages of plant development. Based on their functions and structures, these proteins are divided into three subfamilies (CHD1, CHD3, and CHD7).[26] In *Arabidopsis*, there is one identified CHD1 protein and two CHD3 proteins, while rice has one CHD3 protein identified.[27] Specifically, the *Arabidopsis* CHD1-related gene, CHR5, is activated during embryo development. Mutations disrupt the formation of seed storage proteins and reduce the expression of key embryo regulators such as *LEC1*, *ABI3*, and *FUS3*. Moreover, CHR5 is known to bind to the promoters of *ABI3* and *FUS3*, significantly reducing nucleosome occupancy close to their transcriptional start site.[28] PICKLE (PKL), another important protein, encodes a CHD3 protein that regulates germination by repressing the expression of seed-associated genes through H3K27me3 enrichment. The repression is further enhanced by the plant growth regulator gibberellin (GA).[29] Additionally, PKL and the histone variant, H2A.Z, have opposing roles in maintaining H3K27me3-enriched chromatin.[30] In *Arabidopsis*, CHROMATIN REMODELING4 (CHR4), another member of the CHD3 family, interacts with transcription factors that are crucial for floral meristem identity, influencing the expression of vital floral regulators.[31] In rice, the CHD3 protein, CHR729, significantly influences various aspects of plant development such as early chloroplast architecture in adaxial mesophyll cells, as well as plant height, tillering, panicle size, leaf size, seed germination, and root growth.[32] CHR729 modulates both H3K4 and H3K27 methylation on repressed or tissue-specific genes and plays a role in the gibberellin pathway for development regulation.[32,33] It also affects crown root formation through the auxin pathway, with mutants showing defective crown root development and down-regulation of *OsIAA* genes.[34] Recent studies have further linked CHR729 to the epigenetic regulation of genes involved in oxidative stress responses and wax biosynthesis genes during leaf development.[35,36] These findings highlight the complex and multifaceted roles of CHD proteins in plant development, underscoring the ongoing need to unravel the specific mechanisms by which these proteins influence plant growth and their response to environmental cues.

The primary objective of this research is to functionally characterize BLA1, a CHD3 protein that plays a crucial role in regulating leaf angle and mesocotyl elongation in rice. We used the chemical brassinazole (BRZ) to reduce endogenous BR levels that effectively mitigated the phenotypes associated with the loss of BLA1 function, which were characterized by increased leaf angles and extended mesocotyls. Our findings revealed that BLA1 mutations disrupted the normal patterns of H3K27me3 and H3K4me3 histone modifications at the genomic loci of the BR biosynthesis genes *BRD1* and *D2*. This disruption led to elevated expression levels of these genes, subsequently increasing BR production. The results unveiled a novel epigenetic function of BLA1 (also known as CHR729) in regulating genes essential for BR production in rice, highlighting its critical role in plant development and the potential for manipulating BR pathways for agricultural benefit.

MATERIALS AND METHODS

Plant Materials and Growth Conditions. The *bla1* mutant was identified from a population in which Shuhui527 (SH) mature seeds were treated with ethyl methane sulfonate (EMS). The phenotype of the *bla1* mutant was consistently observed under field and greenhouse conditions in Hangzhou, Zhejiang, China. For this study, all plants were cultivated in the experimental field at the China National Rice Research Institute in Hangzhou. The plants were grown under natural conditions and in a growth chamber that was set to a 14-h light (30 °C)/10-h dark (24 °C) cycle.[37]

Map-Based Cloning. To identify the genomic location of the *BLA1* locus, we crossed the *bla1* mutant with the Japonica variety Nipponbare (NIP for short) and used the resulting F2 population for genetic mapping. A total of 569 individual F2 mutant plants were used for mapping the *BLA1* locus. The *bla1* mutation was identified through PCR amplification of the *BLA1* genomic region from the wild-type and *bla1* mutant plants followed by sequencing.

Mesocotyl Elongation and Emergence Evaluation. The mesocotyl elongation experiment was performed as described previously with some minor modifications.[38] The procedure is as follows. Uniform dehulled rice seeds were first sterilized with 75% ethanol for 5 min, followed by 1% sodium hypochlorite for 10 min. The seeds were then washed three times immediately with sterilized water to remove any residual sterilant. Ten seeds were placed in a test bottle containing half-strength Murashige and Skoog (MS) medium. For plants treated with BRZ, the medium was supplemented with 10 μM BRZ. The seeds were grown for 7 days under controlled conditions. An emergence evaluation was performed according to previous experimental methods. In short, mature seeds were pretreated by soaking on wet gauze for 2 days and sown at a depth of 2 or 5 cm in a soil mixture (three parts nutrient soil to one part vermiculite). All the grooves were exposed to 20,000 lx white fluorescent light for a 14-h light/10-h dark cycle at 30 °C and 75% relative humidity (RH). The emergence of seedlings was recorded daily for 9 days to assess budding conditions.[39]

https://doi.org/10.1021/acs.jafc.4c04248
J. Agric. Food Chem. 2024, 72, 19629−19643

Microscopic Analysis. For cross sections, leaves were sectioned and fixed using 2.5% glutaraldehyde in a fixation buffer (20 mM PIPES, 5 mM $MgCl_2$, 5 mM EGTA, 0.5 mM phenylmethylsulfonyl fluoride, and 1% dimethyl sulfoxide, pH 7.0). The fixed samples were then embedded in Spur's resin, and the sections were cut using a Reichert ultramicrotome. Subsequently, the sections were stained with toluidine blue and observed under a microscope. For transmission electron microscopy observation, leaf samples from both the wild-type and *bla1* mutant were grown under a 14-h light/10-h dark cycle at 30 °C in a growth chamber. Samples were fixed in 2.5% glutaraldehyde in a phosphate buffer at 4 °C for 4 h and then rinsed. Fixed samples were incubated overnight in 1% OsO_4 at 4 °C, followed by an additional 1−2 h of fixation, dehydrated through an ethanol series, and then embedded in Spur's medium. Thin sections were cut and then dual-stained with uranyl acetate and lead citrate. The stained sections were examined using a JEOL JEM-1230 EX electron microscope (JEOL, Japan).[40]

Phylogenetic Analysis. The phylogenetic relationships among proteins from various plant species were investigated to understand their evolutionary history. The methodology used involved the use of protein sequences for species that included *Oryza sativa*, *Theobroma cacao*, and others up to *Aegilops tauschii* that were downloaded from UniProt (https://www.uniprot.org/) and aligned using the Clustal alignment tool, and the evolutionary history was inferred using the neighbor-joining method.[41] The robustness of the tree was tested with 1000 bootstrap replicates.[42] The tree was drawn to scale, where branch lengths correlated with the evolutionary distances measured by the number of amino acid differences per sequence. Distances were computed using the number of differences method. All positions with gaps and missing data were eliminated, with the final data set composed of 1069 positions. Evolutionary analyses were conducted using MEGA5 software.[43]

RNA Extraction and Reverse Transcription and Quantitative Polymerase Chain Reaction (RT-qPCR). Total RNA was extracted from separately sampled leaf and lamina joint regions using TRIzol reagent (Invitrogen, Cat. No. 15596-026, USA). First-strand cDNA was synthesized from isolated RNA using the PrimeScript II first Strand cDNA Synthesis Kit with gDNA remover (TaKaRa, Beijing, China), ensuring the removal of genomic DNA that could interfere with the PCR results. RT-qPCR was performed using SYBR Premix Ex *Taq*II (TaKaRa, Beijing, China) with a CFX96 Real-Time PCR Detection System (Bio-Rad). The rice *OsActin1* gene (LOC_Os03g50885) was used as an internal control to normalize the expression data.[36] Supplementary Table 2 lists the specific primers used for RT-qPCR.

Subcellular Localization. The expression construct, CaMV35S::BLA1::GFP,[44] was transiently introduced into protoplasts isolated from NIP cell suspensions. The transformation was facilitated by polyethylene glycol (PEG) that promoted the uptake of DNA into the protoplasts. After transformation, the protoplasts were incubated for 16 h to allow for adequate expression of the GFP-tagged protein. A confocal laser scanning microscope (LSM 710, Zeiss, Germany) was used to visualize the GFP fluorescence, indicating the location of the BLA1 protein within the cells. To delineate the nuclei, they were stained with 4′,6-diamidino-2-phenylindole (DAPI) that binds strongly to DNA and fluoresces blue under ultraviolet light.[45]

Lamina Inclination Assay. Plants were grown in a controlled environment within a growth chamber and under white light at approximately 20 $\mu mol/m^{-2}$ s^{-1} for a 14-h period and at a temperature of 30 °C. During the dark cycle that lasted 10 h, the temperature was maintained at 25 °C. At 10 days after germination, 1 μL of ethanol containing 10 μM BRZ, a BR biosynthesis inhibitor, was precisely applied to the tips of the lamina of the second leaves. Ethanol serves as a solvent that facilitates the absorption of BRZ into the plant tissue. Following the BRZ treatment, seedlings were allowed to grow under the same conditions for an additional 2 days. Subsequently, the lamina joints of the second leaves were photographed to measure the lamina bending angle.[46]

Endogenous BR Measurement. To assess the concentrations of endogenous BRs in various rice variants (SH, *bla1*, NIP, and *t483*), specific plant tissues, including leaf tissues and lamina joint regions, were systematically sampled. Leaf tissues were collected from each plant type under standardized conditions to ensure consistency across samples. Samples were specifically chosen from similar developmental stages and at the same time of day to minimize variability. The BR levels were quantified using enzyme-linked immunosorbent assays, following a method detailed in a previous study.[47] The assay included three biological replicates per plant type and six technical replicates per biological sample. Data are presented as means ± SD of three biological replicates. A Student *t* test was used to statistically compare the BR concentrations between the wild-type and mutant plants.

Immunoblot Experiments. Plant materials were ground into a fine powder in liquid nitrogen to preserve protein integrity. Proteins were extracted using a buffer containing 50 mM Tris pH 6.8, 4% sodium dodecyl sulfate (SDS), 10% glycerol, 5% 2-mercaptoethanol, and a trace amount of bromophenol blue, along with a complete protease inhibitor from Sigma to prevent protein degradation. The protein concentration was quantified using a Bradford assay, with bovine serum albumin (BSA) serving as the standard. Proteins were separated by electrophoresis on a 10% sodium dodecyl sulfate−polyacrylamide gel electrophoresis (SDS−PAGE) gel. The separated proteins were then transferred onto a nitrocellulose membrane for blotting. The membrane was blocked with 5% milk in tris-buffered saline with TWEEN20 (TBST) (0.8% NaCl, 0.02% KCl, 0.3% Tris, pH 7.4, and 0.05% Tween20) for 30 m at room temperature to prevent nonspecific antibody binding. Primary antibodies were applied and incubated overnight at 4 °C. After washing with TBST, secondary antibodies were applied and incubated for 1 h at room temperature. Blots were developed using the enhanced chemiluminescence (ECL) solutions from Invitrogen to visualize the protein bands.

Chromatin Immunoprecipitation Analysis. Chromatin immunoprecipitation (ChIP) was used to investigate the enrichment of specific histone modifications, H3K4me3 and H3K27me3, in the rice lamina joint regions. The methodology was adapted from a previously published protocol.[48] Simply, approximately 2 g of tissue was harvested and cross-linked using 1% formaldehyde under a vacuum for 15 m to fix the proteins to the DNA. The cross-linked chromatin was fragmented to an average size of 200−500 bp using sonication. Fragmented chromatin was incubated with antibody-coated beads overnight to isolate complexes with H3K4me3 and H3K27me3 modifications. The specific antibodies used included Anti-H3K4me3 from Abcam (ab8580) and Anti-H3K27me3 from Millipore (07-449). Following the immunoprecipitation, cross-links were reversed, and DNA was purified. Real-time PCR was performed to quantify the enrichment of each histone modification. Enrichment was calculated using the equation $2^{(\text{Ct of input}-\text{Ct of sample ChIP})}$ that normalizes the threshold cycle (Ct) of the ChIP sample to that of the input DNA. Supplementary Table 2 lists the specific primers used for real-time PCR.

Yeast One-Hybrid Assay. *BLA1* was segmented into three fragments based on its conserved domains. Each fragment was then cloned into the pGADT7 vector using double-enzyme digestion with EcoR I and BamH I. The promoters of *BRD1* (595 base pairs) and *D2* (577 base pairs) genes were cloned and separately recombined into the pAbAi vector. Using the Matchmaker Gold Yeast One-Hybrid Library Screening System (TaKaRa), the linearized plasmids pAbAi-BRD1 and pAbAi-D2 were introduced into the yeast strain, Y1H Gold, and the yeast was cultured on SD/-Ura agar plates to select the successful transformations. Yeast cultures were screened on SD/-Ura/AbA plates with aureobasidin A (AbA) concentrations of 600 and 1000 ng/ml to determine the minimum concentration that inhibited yeast growth. Subsequently, the pGADT7-BLA1-1, -2, -3 plasmids were transformed into yeast strains already harboring pAbAi-BRD1 or pAbAi-D2. The transformed yeast strains were then plated successively on SD/-Leu and SD/-Leu/AbA media. Yeast growth at 30 °C was monitored to assess protein−DNA interactions. Supplementary Table 2 shows the primers.

Data Processing and Analysis. All data were statistically analyzed and plotted using GraphPad Prism 9 software (San Jose,

https://doi.org/10.1021/acs.jafc.4c04248
J. Agric. Food Chem. 2024, 72, 19629−19643

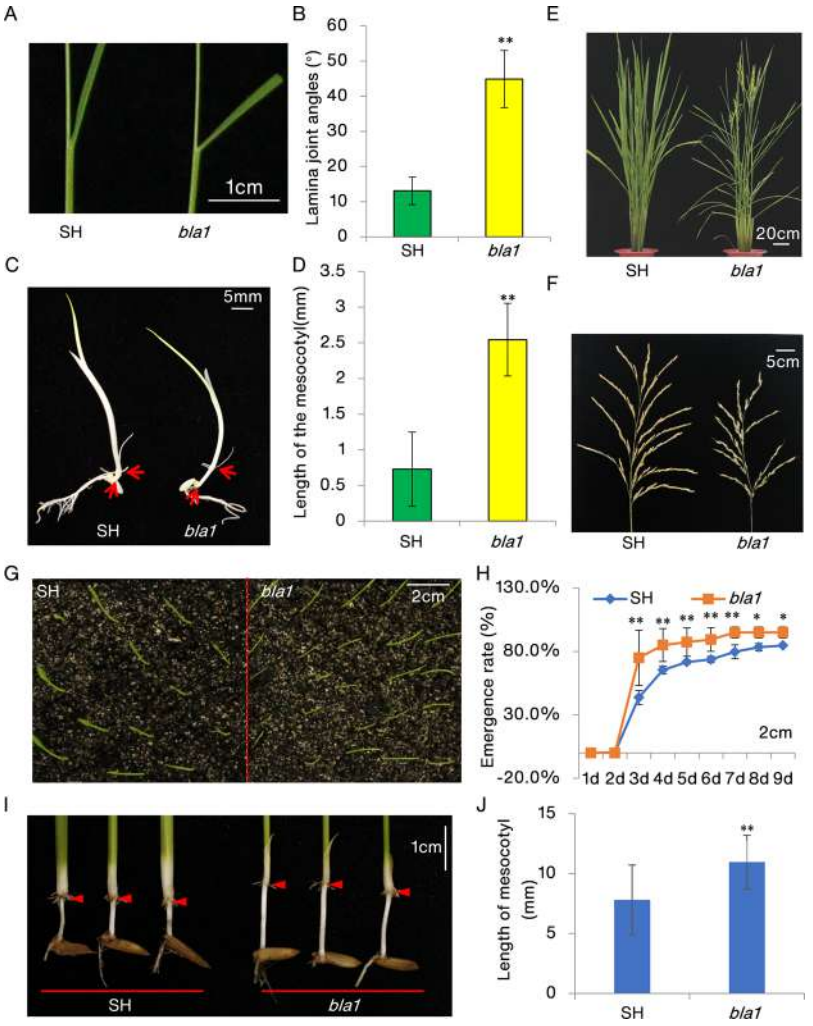

Figure 1. Phenotypic characterization of the wild-type (WT) and *bla1* mutants. (A) Lamina joint images of the wild-type (SH) and *bla1* mutant plants displaying the significantly increased leaf angle in the mutant plant. Scale bars = 1 cm. (B) Measurements of the lamina joint angles of the wild-type and *bla1* seedlings. Data presented are means from 30 plants. Statistical analysis was performed using Student's *t* test. $^{**}P < 0.01$. (C) Mesocotyls of the etiolated seedlings of the *bla1* mutants were longer than those of the wild-type (SH) under continuous darkness for 7 days. Arrows indicate the mesocotyls. Scale bar = 5 mm. (D) Measurements of the mesocotyl lengths of the wild-type and *bla1* seedlings. Data presented are means from 50 plants. A statistical analysis was performed using Student's *t* test. $^{**}P < 0.01$. (E) Phenotypes of the wild-type and *bla1* seedlings cultured in the field at the booting stage. Scale bar = 20 cm. (F) Phenotypes of the spikes of the wild-type and *bla1* plants. Scale bar = 5 cm. (G) *bla1* mutants emerged faster than the SH plants. Photograph captured on the fourth day after sowing in 2-cm-deep soil. (H) Dynamic emergence rates of the *bla1* mutants and SH recorded for 9 days after sowing under 2 cm soil. Statistical analysis was performed using Student's *t* test. Means ± SD are given in H ($n = 3$). $^{*}P < 0.05$ and $^{**}P < 0.01$. (I) Phenotypes of the mesocotyl of the SH and *bla1* plants. (J) Mesocotyl lengths. Statistical analysis was performed using Student's *t* test. Data are presented as means ± SD ($n = 30$). Error bars indicate standard deviations. $^{*}P < 0.05$ and $^{**}P < 0.01$.

CA, USA). Statistical significance was assessed using Student's *t* test. A *p*-value < 0.05 indicated a significant difference. All results are expressed as mean values ± standard errors (SE). The different letters indicate a significant difference ($p < 0.05$, one-way analysis of variance (ANOVA)).

Accession Numbers. Sequence data from this article can be found in the GenBank data libraries under the following accession numbers: *BLA1*, LOC_Os07g31450; *OsBRI1(D61)*, LOC_Os01g52050; *D2*, LOC_Os01g10040; *D11*, LOC_Os04g39430; *OsCPD1*, LOC_Os11g04710; *BRD1*, LOC_Os03g40540; *BRD2*, LOC_Os10g25780; *DSG1*, LOC_Os06g06090; *BAK1*, LOC_Os08g07760; *LIC1*, LOC_Os06g49080; *ILI1*, LOC_Os04g54900; *BU1*, LOC_Os06g12210; *RAVL1*, LOC_Os04g49230; *GSK1*, LOC_Os01g10840; *BLE2*, LOC_Os07g45570; *OsActin1*, LOC_Os03g50885; and *OsActin7*, LOC_Os11g06390.

RESULTS

Phenotypic Characterization of the *bla1* Mutant. To explore the molecular mechanism of BR biosynthesis in rice, we screened the library of EMS-induced mutants for variations in the lamina joint bending angles. The *bla1* mutant, characterized by a larger leaf angle than its wild-type, Shuhui527 (SH), was identified. Throughout all developmental stages, the *bla1* mutant exhibited a significantly larger leaf angle than the wild-type (Figure 1A,B,E). Under total darkness, the mesocotyl elongation of rice was enhanced, mirroring the dependency on BR seen in *Arabidopsis* hypocotyl elongation.[49,50] We compared the mesocotyl elongation of the wild-type and *bla1* mutant seedlings that germinated in the half-strength MS medium under dark conditions, and the

https://doi.org/10.1021/acs.jafc.4c04248
J. Agric. Food Chem. 2024, 72, 19629−19643

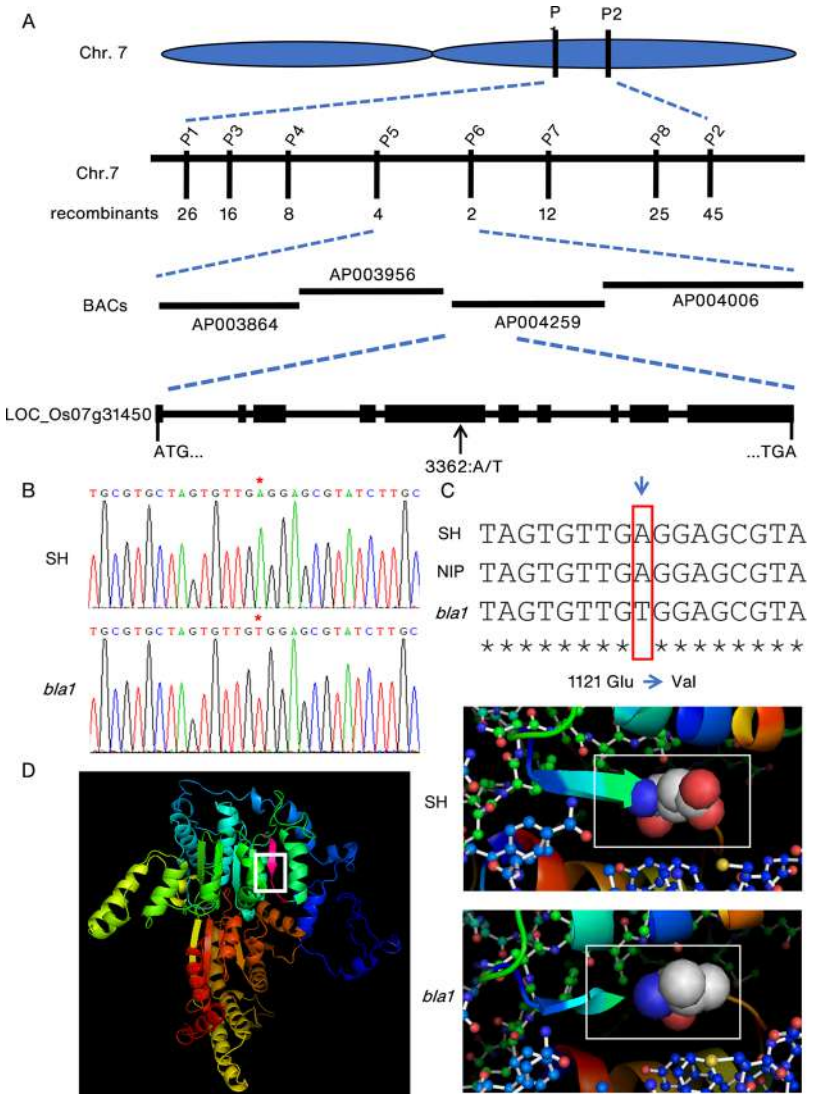

Figure 2. Cloning of *BLA1*. (A) *bla1* was mapped initially to the middle of rice chromosome 7 between markers P5 and P6. Fine-mapping was performed to narrow down *bla1* to a region in AP004259. Mutation sites were found in *BLA1*. (B) Comparison of the sequencing results of *bla1* and the WT (SH). The red stars represent the mutation site. (C) Sequences of SH, NIP, and *bla1*. (D) Structures of BLA1 in the WT (SH) and *bla1* were predicted using standard template-based modeling. White boxes indicate the mutation sites.

findings showed that the *bla1* mutant's mesocotyl length was longer than that of the wild-type plant (Figure 1C,D).

Additionally, the humus soil culture method was used to measure the mesocotyl length of both the wild-type and *bla1* mutant. The wild-type and mutant seeds were sown at a soil depth of 2 cm, and the emergence rates were observed for 9 days. The seeds showing identical buds were selected to eliminate the influence of varied germination speeds. The results showed that the *bla1* mutant seedlings showed faster and more consistent growth than the wild-type, although both groups ultimately showed similar emergence rates. Under the same soil conditions, the *bla1* mutants consistently had longer mesocotyls than the wild-type counterparts (Figure 1I,J).

Moreover, the mutant showed several other growth defects, including adaxial albino and narrower leaves at all growth stages (Figure S1A−D). In contrast to the wild-type, the mutant *bla1* exhibited a noticeably reduced rate of germination (Figure S1F). At maturity, the mutant was shorter with fewer and smaller panicles and shorter seeds than the wild-type (Figures 1F and S1E; Table S1). According to an analysis of the leaf cross-sections from the wild-type and *bla1* plants, the majority of cells in the mutant leaves on the adaxial side lacked chlorenchyma (Figure S1G,H). Transmission electron microscopy (TEM) studies revealed that while the wild-type leaves had well-developed chloroplasts in the membrane structures and densely packed thylakoids (Figure S2A−C), the mutant leaves displayed abnormal chloroplast shapes with loose thylakoid membranes and less dense grana stacks on the adaxial side (Figure S2D,F). On the abaxial side, there were no appreciable variations in chloroplast ultrastructures between the wild-type and *bla1* mutant (Figure S2G−I).

Map-Based Cloning of the *BLA1* Gene. For the genetic analysis of the *bla1* mutant, we conducted a cross between *bla1* and NIP (a Japonica variety). The segregation ratio in F2 plants was approximately 3:1, suggesting that the mutant's phenotypic abnormalities are controlled by a single recessive nuclear gene. We used map-based cloning to isolate the *BLA1* gene (Figure 2A), initially localizing it between markers P1 and P2 on the long arm of chromosome 7 using 24 F2 plants homozygous for *bla1*. Further mapping with additional F2

https://doi.org/10.1021/acs.jafc.4c04248
J. Agric. Food Chem. 2024, 72, 19629−19643

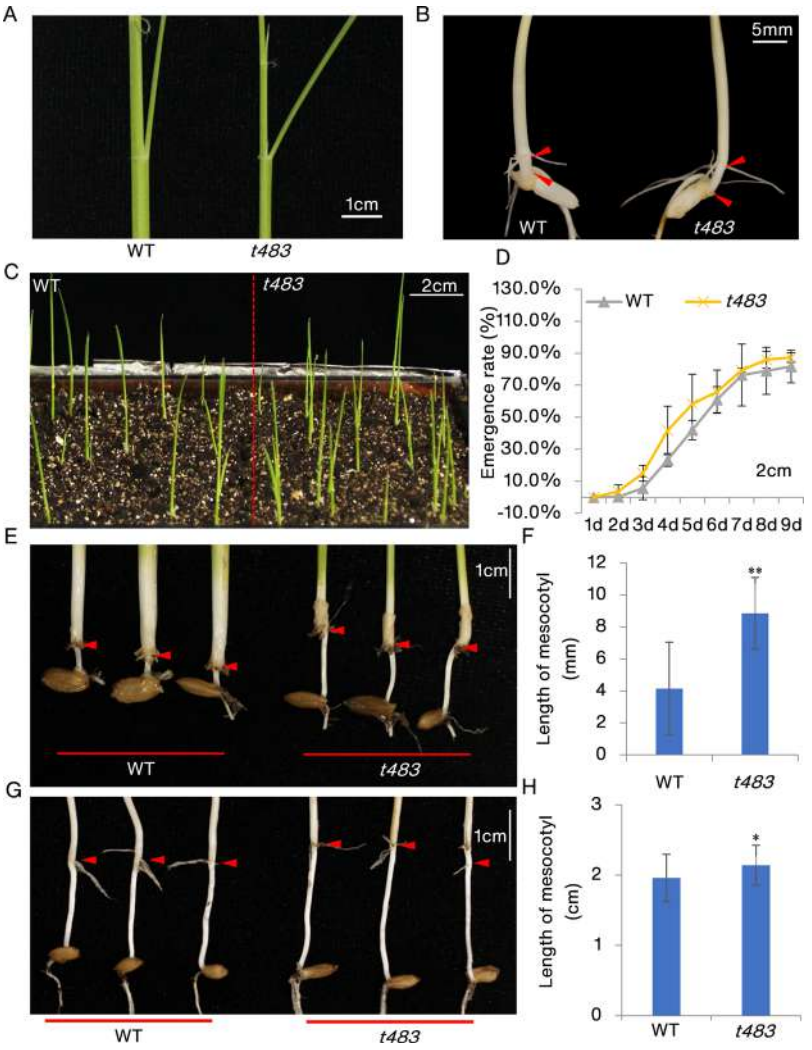

Figure 3. Phenotypic characterization of the wild-type (WT) and *t483* mutants. (A) Lamina joint images of the wild-type and *t483* mutant plants showing significantly increased leaf angles in the mutant plant. Scale bars = 1 cm. (B) Mesocotyls of the etiolated seedlings of the *t483* mutants were longer than those of the WT under continuous darkness for 7 days. Arrows indicate the mesocotyls. Scale bar = 5 mm. (C) *t483* mutants emerged faster than the WT plants. Photograph captured on the fourth day after sowing in 2 cm deep soil. (D) Dynamic emergence rates of the *t483* mutants and WT recorded for 9 days after sowing under 2 cm soil. (E) Phenotypes of the mesocotyls of the WT and *t483* plants under 2 cm soil. (F) Mesocotyl lengths under 2 cm soil. (G) Phenotypes of the mesocotyls of the WT and *t483* plants under 5 cm soil. (H) Mesocotyl lengths under 5 cm soil. Data are presented as means ± SD (n = 30). Error bars indicate standard deviations. $^{**}P < 0.01$ and $^{*}P < 0.05$.

plants refined the location to a region between the SSR markers P5 and P6. A sequence analysis within this region revealed a single nucleotide substitution (A-to-T) in LOC_Os07g31450 at the fifth exon, 3362 bp downstream from the start codon. This mutation likely changes amino acid 1121 from glutamate (E), a conserved residue, to valine (V) (Figure 2B,C). Further investigation of the rice genome database indicated that LOC_Os07g31450 includes ten exons and nine introns and encodes a chromatin-remodeling factor (OsCHR4) that consists of 2259 amino acids. This protein had been noted in previous studies as LOC_Os07g31450[32−36,44] and identified as a potential candidate gene for *BLA1*.

The 3D structure of BLA1 was modeled using SWISS-MODEL, a standard template-based approach. BLA1 is composed of multiple functional domains: a plant homeodomain (PHD) zinc finger domain, two chromo domains, an SNF2-related helicase domain, and a DNA binding domain. Within the DNA binding domain, the glutamate residue at position 1121 (E1121) was found to be critical. The investigation indicated that the substitution of glutamate at this position with valine (E1121V) might alter the protein's structural integrity by modifying the charge and hydrophilic characteristics at this junction (Figure 2D). Given that Val is hydrophobic and Glu is a hydrophilic residue, the change from hydrophilic amino acids into hydrophobic amino acids may affect how the protein dissolves and folds correctly by altering its affinity ability for water molecules. However, the Glu acidic amino acid contains a negatively charged $-CH_2)_2-COO-$ side chain, and the nonpolar Val amino acid has side chains of −H and −CH3. Consequently, the substitution of Glu1121Val alters this protein's charge characteristics, and this may affect its hydrophilicity, charge properties, and overall structure.

Verification and Evolutionary Analysis of BLA1. To further validate the role of BLA1 in the phenotypes, such as increased leaf angles and dark-induced mesocotyl elongations, we examined the *t483* mutant. This mutant carries a single nucleotide substitution (T to A) in the gene LOC_Os07g31450 at 2701 bp downstream of the start codon

https://doi.org/10.1021/acs.jafc.4c04248
J. Agric. Food Chem. 2024, 72, 19629−19643

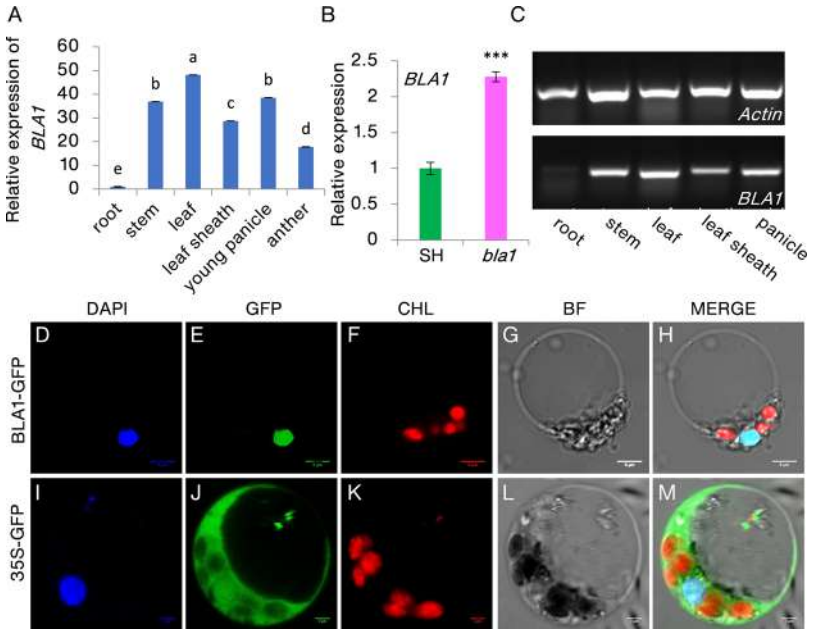

Figure 4. Expression pattern and intracellular localization of BLA1. (A) Analysis of the expression of *BLA1* in various organs using RT-qPCR. All the materials were harvested from a mature WT plant. *OsActin1* was used as the internal control. Data are presented as means ± SD (n = 3). Different lowercase letters indicate statistically significant differences ($P < 0.05$, one-way ANOVA). (B) Expression of *BLA1* in the wild-type (SH) and *bla1* mutant. Data are presented as means ± SD (n = 3). Error bars indicate standard deviations. ***$P < 0.001$. (C) Analysis of the expression of *BLA1* in various organs using a semiquantitative PCR assay. (D−H) Subcellular localization of BLA1. (D) DAPI staining. (E) Binary vector containing 35S::BLA1-GFP was transiently expressed in the rice protoplasts. (F) Autofluorescence chlorophyll (red), (G) bright field, (H) merged image, and (I) DAPI staining. (J) Binary vector containing 35S::GFP was transiently expressed in the rice protoplasts. (K) Autofluorescence chlorophyll (red), (L) bright field, and (M) merged image. Scale bars = 2 μm.

in the fifth exon, introducing an early stop codon (Figure S3A,B).[32] Like the *bla1* mutant, the *t483* mutant exhibited greater leaf angles than the wild-type in both seedling and mature plants in a field condition (Figures 3A and S3C), as well as increased mesocotyl elongation (Figure 3B). Emergence rate experiments further demonstrated that seedlings of the *t483* mutant had a higher emergence rate than the wild-type when covered with 2 cm of soil, and this was particularly noticeable between the fourth and fifth days after planting, although rates eventually converged (Figure 3C,D). Under both 2 and 5 cm of soil cover, the mesocotyls of the *t483* mutants were significantly longer than those of the wild-types (Figure 3E−H). Additionally, the complementary plants carry a pCAMBIA1300::GFP plasmid containing 3,096-bp promoter of *BLA1* and a 6,857-bp cDNA fragment, with higher expression level of *BLA1* than the wild-type plants (especially the C1 line), showed significantly lower emergence rates than that of the wild-type (Figure S4). Moreover, another allelic mutant of the *BLA1* gene, (*crl6*), reported by Wang et al., displayed larger flag leaf angles than the wild-type.[34] These findings collectively confirm that mutations in *BLA1* are linked to the phenotypic changes observed in the *bla1* mutant, particularly in terms of leaf angles and mesocotyl elongation.

To explore the evolutionary relationships and sequence conservation of the BLA1 protein among plants, we used protein sequence comparison techniques, including the neighbor-joining tree method (Figure S5A). A phylogenetic analysis revealed that the BLA1 protein is highly conserved among gramineous plants such as *Zea mays*, *Sorghum bicolor*, *Oryza brachyantha,* and *Triticum urartu*, forming a distinct clade separate from other plant species. Within this clade, the rice BLA1 aligned closely with *O. brachyantha* and *Brachypodium distachyon*, and other plant species were primarily divided into monocotyledons and dicotyledons subfamilies. Through a sequence alignment, the E1121 site was identified as highly conserved across all examined sequences, underscoring its critical role in the function of the CHR4 protein (Figure S5B).

Expression Pattern and Subcellular Localization of BLA1. To elucidate the expression pattern of *BLA1*, RT-qPCR analysis (using *OsActin1* and *H3* genes as internal control) were conducted on the total RNA extracted from various organs of the wild-type plants: the roots, stems, leaves, leaf sheaths, and panicles. The analysis revealed that *BLA1* was expressed in all the samples, with the highest level of expression occurring in the leaves during the seedling stage. It was also found to be highly expressed in other tissues (Figures 4A and S6). This expression pattern was further supported by semiquantitative PCR that confirmed the constitutive expression of *BLA1* across the different rice tissues (Figure 4C). A notable variance in *BLA1* expression between the leaf blades of the wild-type and *bla1* mutant suggested a feedback regulation at the RNA level, possibly triggered by the single amino acid mutation (Figures 4B and S6).

Following the determination of *BLA1*'s expression profile, we assessed its subcellular localization in rice cells through transient transformation assays using protoplasts. The constructed CaMV35S::OsCHR4::GFP and control 35S::GFP were introduced into the rice protoplasts. The fluorescence of BLA1-GFP colocalized with the DAPI-stained nuclei indicated its nuclear localization (Figure 4D−H). In contrast, the GFP signal from the 35S::GFP vector control was distributed ubiquitously throughout the cells (Figure 4I−M). These observations confirm that BLA1 predominantly

https://doi.org/10.1021/acs.jafc.4c04248
J. Agric. Food Chem. 2024, 72, 19629−19643

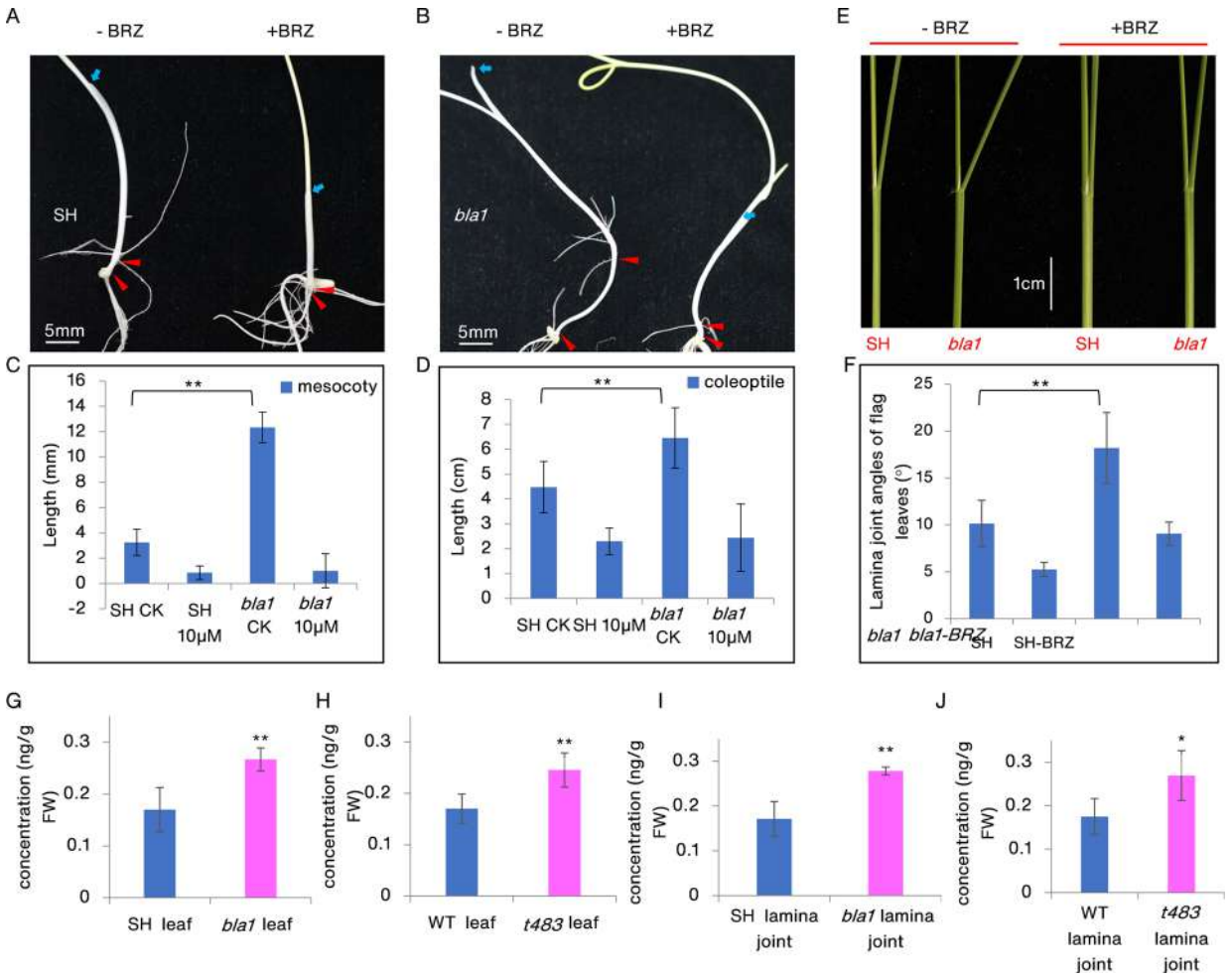

Figure 5. Phenotype of the *bla1* mutant rescued by BRZ treatment and the detection of endogenous BR. (A) Mesocotyls of the etiolated seedlings of the wild-type (SH) with and without 10 μM BRZ under continuous darkness for 7 days. Red and blue arrows indicate mesocotyls and coleoptiles, respectively. Scale bar = 5 mm. (B) Mesocotyls of the etiolated seedlings of *bla1* with and without 10 μM BRZ under continuous darkness for 7 days. Red and blue arrows indicate mesocotyls and coleoptiles, respectively. Scale bar = 5 mm. (C) Mesocotyl lengths of the SH and *bla1* mutant with and without BRZ treatment. (D) Coleoptile lengths of the SH and *bla1* mutant with and without BRZ treatment. (E,F) Lamina joints of the wild-type and *bla1* mutant plants with and without BRZ treatment. Scale bars = 1 cm. (G) Quantification of the endogenous BR contents of the SH and *bla1* mutant in leaves. (H) Quantification of the endogenous BR contents of the WT and *t483* mutant in leaves. (I) Quantification of the endogenous BR contents of the SH and *bla1* mutant in lamina joint regions. (J) Quantification of the endogenous BR contents of the WT and *t483* mutant in lamina joint regions. Data are presented as means ± SD (n = 30). Error bars indicate standard deviations. $^{**}P < 0.01$ and $^{*}P < 0.05$.

localized to the nucleus, aligning with its presumed role in chromatin remodeling.

BLA1 Was Involved in BR Biosynthesis, Not BR Signaling. The role of BLA1 in rice BR biosynthesis rather than BR signaling was investigated by examining its effect on plant growth under different conditions. To discern between BR-deficient and BR-insensitive mutants, we used the sensitivity of rice lamina joint bending to BRs and the inhibition of mesocotyl and coleoptile elongation by BRZ under a dark condition. In the absence of BRZ, a BR synthesis inhibitor, the wild-type plants displayed normal elongation of mesocotyls and coleoptiles in a half-strength MS medium under dark conditions. Upon application of 10 μM BRZ, growth of these tissues was notably suppressed (Figure 5A,C,D), agreeing with the expected outcomes for BR synthesis inhibition. In contrast, the *bla1* mutant exhibited significant elongation of mesocotyls and coleoptiles in the absence of BRZ, surpassing wild-type growth levels. When treated with 10 μM BRZ, the elongation of mesocotyls and coleoptiles in the *bla1* mutant reverted to levels comparable to the wild-type, indicating the suppression of an enhanced BR biosynthesis pathway (Figure 5B−D). Additionally, when BRZ was applied directly to the lamina tips of 10-day-old seedlings, the bending angle of the second leaves in the *bla1* mutant decreased markedly, resembling that of the wild-type (Figure 5E,F). Similar to *bla1*, the *t483* mutant displayed corrective responses in mesocotyl elongation and lamina bending angles upon BRZ treatment (Figure S7). Notably, mutants known to be involved in BR signaling did not exhibit changes in mesocotyl and coleoptile length when treated with BRZ,[51] which supported the notion that the phenotypic changes in *bla1* were due to increased endogenous BR synthesis rather than defects in the BR signaling pathways.

To further substantiate this hypothesis that the *BLA1* mutation influences BR biosynthesis, we measured the endogenous BR concentrations in both the wild-type and mutant plants, focusing on leaves and lamina joint regions. The wild-type plants exhibited a baseline BR content of

https://doi.org/10.1021/acs.jafc.4c04248
J. Agric. Food Chem. 2024, 72, 19629−19643

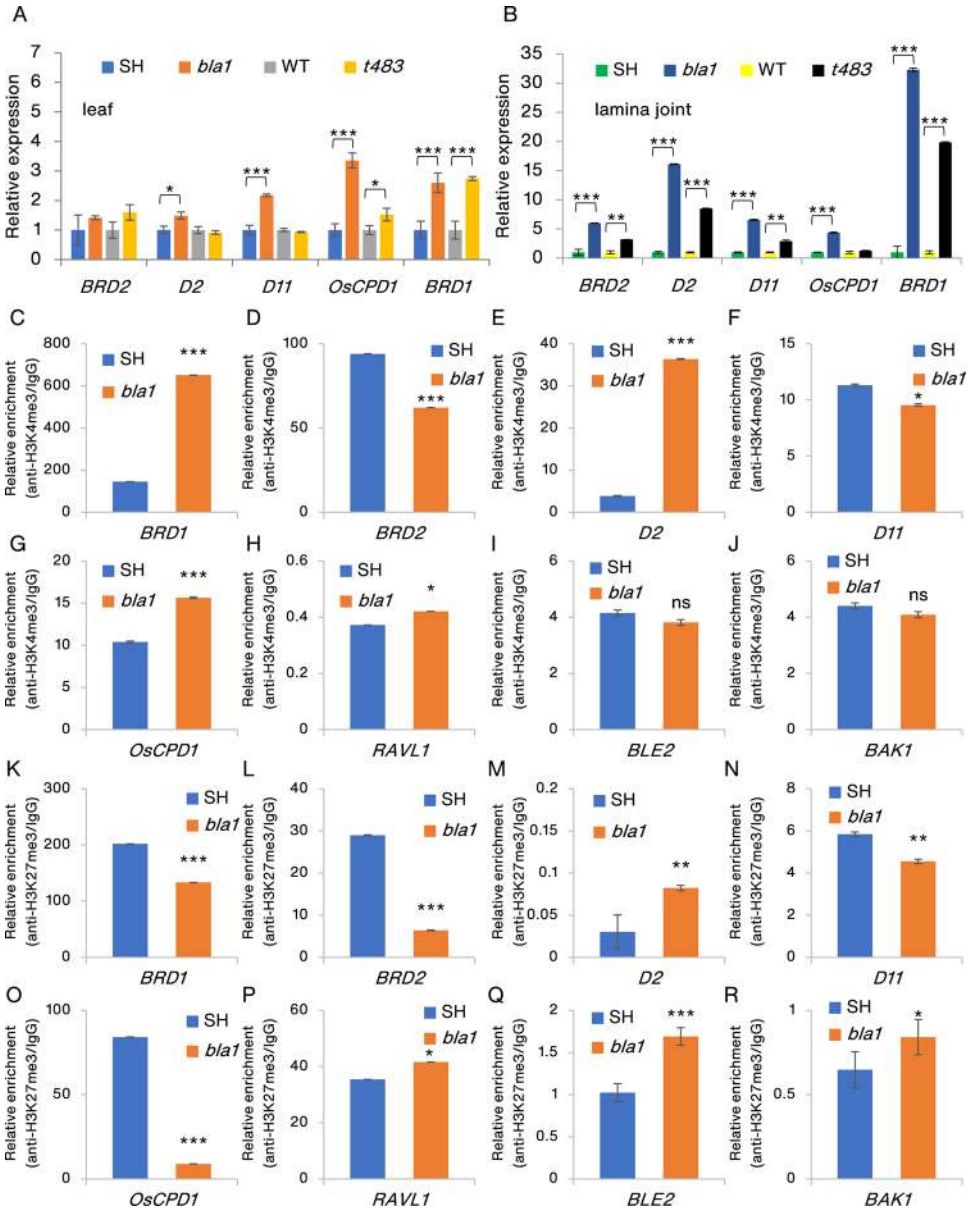

Figure 6. BLA1 regulates the expression of genes related to BR biosynthesis. (A) Relative expression levels of *BRD2*, *D2*, *D11*, *OsCPD1*, and *BRD1* in leaves of the SH, *bla1*, WT, and *t483* plants. (B) Relative expression levels of *BRD2*, *D2*, *D11*, *OsCPD1*, and *BRD1* in the lamina joint regions of the SH, *bla1*, WT, and *t483* plants. (C−R) ChIP-qPCR analysis of the enrichment of H3K4me3 (C−J) and H3K27me3 (K−R) on BR synthesis and signaling genes in the *bla1* mutant relative to the WT. *OsActin7* was used for the normalization of the qPCR analysis. Data are presented as means ± SD. Error bars indicate standard deviations. $^{*}P < 0.05$, $^{**}P < 0.01$, and $^{***}P < 0.001$.

approximately 0.16964 ng/g fresh weight in the leaves. In contrast, the *bla1* mutant showed a significantly increased concentration of 0.266802 ng/g fresh weight, highlighting a substantial enhancement in BR synthesis (Figure 5G). Similarly, in the lamina joint regions, the wild-type plants maintained a BR level of 0.170135 ng/g fresh weight, while the *bla1* mutant had a notably higher content of 0.278368 ng/g fresh weight, further supporting the enhanced BR biosynthetic activity in this mutant (Figure 5I). These patterns of increased BR concentrations were also significantly observed in the *t483* mutant allele that shares the *BLA1* mutation (Figure 5H,J). These results conclusively indicate that mutations in the *BLA1* gene led to an upregulation of BR biosynthesis in rice. The elevated endogenous BR levels in the *bla1* and *t483* mutants correlated strongly with the observed phenotypic manifestations, such as increased leaf angle and mesocotyl elongation. This enhanced BR production was likely responsible for the distinct growth characteristics seen in these mutants, confirming the crucial role of the *BLA1* gene in the BR biosynthesis pathway rather than in the signaling mechanisms.

Histone Modification of the BR Biosynthesis-Related Gene Was Affected in *bla1*. To investigate the increased endogenous BR output in the *bla1* and *t483* mutants, we analyzed the expression levels of genes involved in BR biosynthesis: *D2*, *D11*, *BRD1*, *BRD2*, and *OsCPD1*. A RT-qPCR analysis was conducted on RNA extracted from leaves and lamina joint regions of the 30-day-old plants. The analysis revealed a significant upregulation of *BRD1* and *D2* transcripts in the lamina joint regions of both the *bla1* and *t483* mutants compared with the wild-type plants, with a slight increase also

https://doi.org/10.1021/acs.jafc.4c04248
J. Agric. Food Chem. 2024, 72, 19629−19643

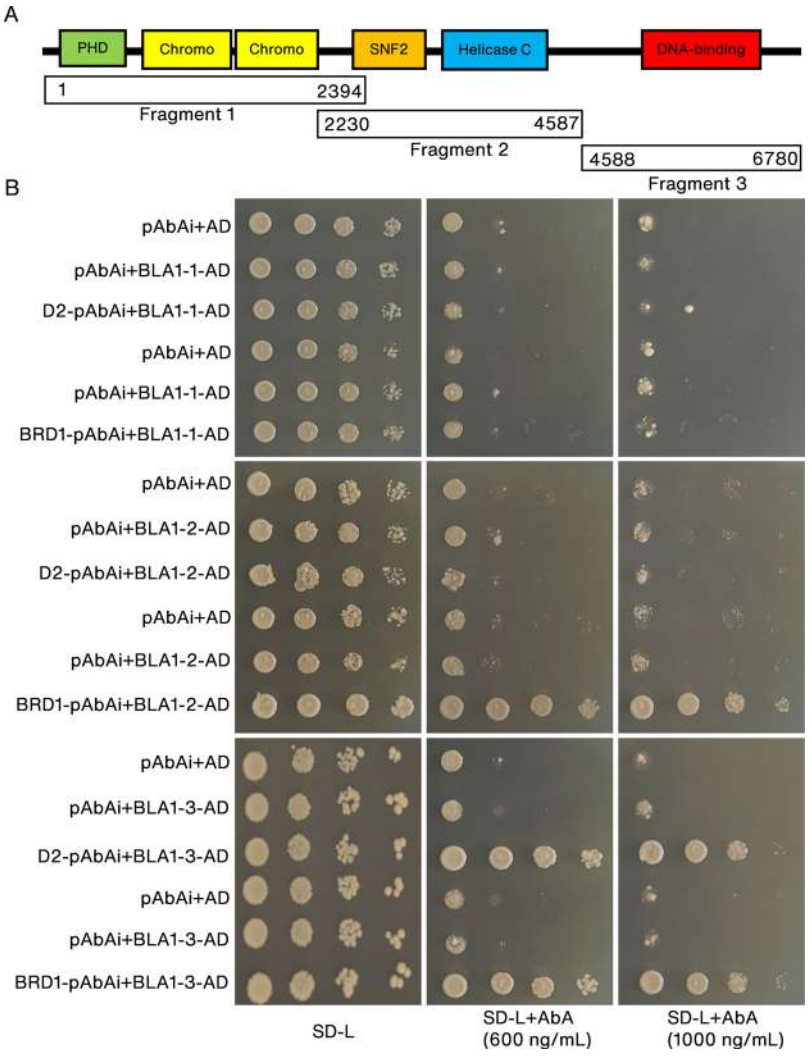

Figure 7. BLA1 binds with *BRD1* and *D2* promoters. (A) Diagram of the BLA1 protein domain. (B) Yeast one-hybrid (Y1H) assays showing the interactions between BLA1 and the *BRD1* and *D2* promoters. pAbAi + pGADT7 and pAbAi + BLA1-pGADT7 were used as the negative controls.

observed in leaves (Figures 6A,B and S8A,B). The expression levels of *BRD2*, *D11*, and *OsCPD1* showed only minor increases in the lamina joint regions (Figure 6B). However, these genes showed a decreasing trend in complementary lines (Figure S9). In contrast, BR signaling genes did not show consistent changes across the mutants (Figure S8C). Notably, *BLA1* expression was similar between each of the BR signaling mutants and the wild-type plants (Figure S8D,E), suggesting that BLA1's functional deficiency affected BR biosynthesis predominantly by modulating the expression of specific biosynthetic genes, particularly *BRD1* and *D2*.

Previous studies have shown that histone methylation states, such as trimethylation of histone lysine 4 (H3K4me3) associated with gene activation and lysine 27 (H3K27me3) with suppression, are crucial for gene regulation.[29,52] The rice CHD3 protein OsCHR4, identified as a chromatin remodeler, regulates gene expression by modulating levels of H3K4me3 and H3K27me3.[53] We investigated changes in these histone modifications in the *bla1* mutant by isolating histones from the leaves and lamina joint regions of the 3-week-old SH, *bla1*, Nip, and *t483* plants and performing Western blot analysis with specific antibodies. The results indicated a global reduction in both H3K4me3 and H3K27me3 in the *bla1* and *t483* mutants compared with their respective wild-type controls (Figure S10), suggesting a role for BLA1 in modifying histone methylation at a key genomic region.

Given these findings, we hypothesized that BLA1 might influence the transcription of BR biosynthesis genes by altering H3K4me3 and H3K27me3 depositions. ChIP assays using specific antibodies for these modifications, followed by qPCR analysis of the 5′ end regions of the biosynthetic genes, showed significant changes in the enrichment of H3K4me3 and H3K27me3 (Figure 6C−R). Importantly, *BRD1* and *OsCPD1* showed increased H3K4me3 and decreased H3K27me3 levels (Figure 6C,G,K,O), suggesting an activation of these genes. In contrast, *BRD2* showed a decrease in both H3K27me3 and H3K4me3 (Figure 6D,L), while *D2* exhibited a substantial increase in H3K4me3 and H3K27me3 in the *bla1* mutant (Figure 6E,M). Other genes related to BR signaling did not show significant methylation changes (Figure 6F,H−J,P−R). Additionally, two downregulated genes in the *bla1* mutant (LOC_Os12g10630 and LOC_Os08g36110) displayed decreased levels of H3K4me3 and H3K27me3 (Figure S11A−F), which was consistent with previous reports[33] and demonstrated the reliability of our ChIP-qPCR results. Thus, it was concluded that BLA1 likely exerts its effects on histone modifications associated with BR biosynthesis genes, especially

https://doi.org/10.1021/acs.jafc.4c04248
J. Agric. Food Chem. 2024, 72, 19629−19643

in *BRD1* and *D2*, thereby epigenetically regulating their expression.

To confirm BLA1's role in regulating BR biosynthesis genes, we conducted a yeast one-hybrid (Y1H) assay using the promoter regions of *BRD1* and *D2* as bait. Fragments of BLA1 containing its functional domains were tested for interaction in the Y1H system (Figure 7A). As depicted in Figure 8, all clones were able to grow on SD/-Leu plates. However, only the yeast strains transformed with pGADT7-BLA1−2/pAbAi-BRD1, pGADT7-BLA1−3/pAbAi-BRD1, and pGADT7-BLA1−3/pAbAi-D2 were able to survive on the medium supplemented with 600 or 1000 ng/mL AbA, while the negative controls failed to grow (Figure 7B), further confirming the binding ability of BLA1 to the promoter regions of *BRD1* and *D2*. This evidence further supports the regulatory role of BLA1 in BR biosynthesis through epigenetic modulation of key biosynthetic genes.

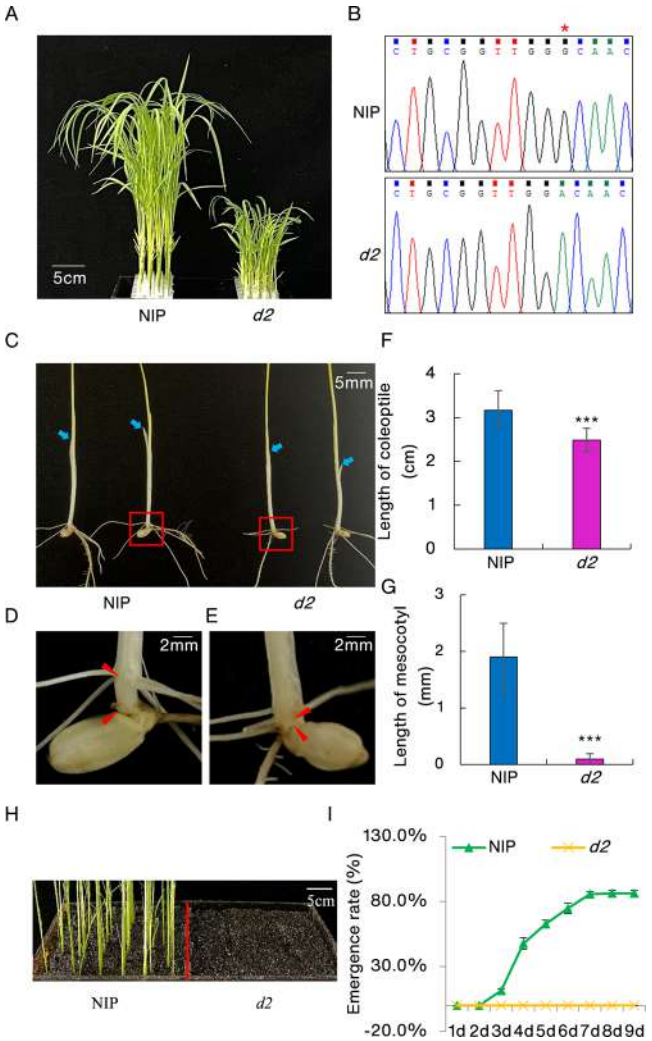

Figure 8. Phenotypic characterization of the wild-type (NIP) and *d2* mutants. (A) Phenotypes of the 15-day-old WT and *d2* plants. Scale bars = 5 cm. (B) Sequencing confirmation of the *D2* gene in *d2* plants. (C) Photomorphogenic phenotype of *d2* grown in the dark. Scale bars = 5 mm. (D,E) Close-up of the boxed region in (C), scale bar = 2 mm. (F) Coleoptile lengths of NIP and *d2* under continuous darkness for 7 days. (G) Mesocotyl lengths of NIP and *d2* under continuous darkness for 7 days. (H) *d2* mutants emerged slower than the WT plants. Photograph captured on the ninth day after sowing in 5 cm deep soil. (I) Dynamic emergence rates of the *d2* mutants and WT recorded for 9 days after sowing under 5 cm soil. Red triangles and blue arrows indicate mesocotyls and coleoptiles, respectively. Data are presented as means ± SD (n = 40). Error bars indicate standard deviations. ***P < 0.001.

D2 Acted Downstream of BLA1 to Regulate Mesocotyl Elongation and the Emergence Rate. Given that BLA1 binds to the promoter regions of *BRD1* and *D2*, we asked whether D2 is the downstream player of BLA1. We used a *d2* mutant that has a single nucleotide base change at the coding sequence (CDS) that results in the conversion of glycine to aspartic acid (Figure 8A,B). We then conducted mesocotyl elongation and emergence rate assays. Under dark conditions, the wild-type plants displayed significant mesocotyl elongation, achieving nearly 2 mm of length on the 1/2 strength MS medium, while the *d2* mutant showed no such elongation (Figure 8C−E,G). Additionally, under dark conditions, the coleoptiles of the *d2* mutant were notably shorter than those of the wild-type (Figure 8F). In addition, the emergence rate experiments revealed that when planted under 5 cm of soil, the *d2* mutant seedlings exhibited a substantially lower emergence rate than the wild-type seedlings. By the seventh day, while nearly 90% of the wild-type seedlings had emerged, the *d2* mutant displayed no emergence at all (Figure 8H,I). The lack of mesocotyl and coleoptile elongation in the *d2* mutant suggested a significant disruption in BR biosynthesis that led to impaired growth under soil cover.

These observations collectively indicate that BLA1, potentially via its regulation of BR synthesis genes such as *D2* and *BRD1*, played a fundamental role in controlling the elongation processes of mesocotyls and coleoptiles. This regulatory mechanism is essential for optimal seedling emergence and early plant development, emphasizing the interplay between genetic regulation and hormone biosynthesis pathways in plant physiology.

DISCUSSION

In this study, we have delineated the specific roles of CHR729 and its allelic mutants in regulating BR biosynthesis via epigenetic modifications, a process less understood in rice compared with other plant models. Unlike other CHD proteins, CHR729, particularly through its BLA1 variant, played a pivotal role in modulating histone methylation patterns at key BR synthesis genes such as *BRD1* and *D2*. The upregulated expression of these genes in the *bla1* mutants correlated with increased BR levels that directly contribute to phenotypic traits such as increased leaf angles and mesocotyl elongation. These findings not only advance our understanding of the functions of the CHD protein in chromatin dynamics but also suggest potential genetic targets for enhancing crop resilience and growth characteristics under variable environmental conditions. Further studies should explore the full spectrum of genes regulated by BLA1 and investigate the potential coregulation of these genes with other epigenetic modifications to fully elucidate the chromatin-based regulatory networks in plant development.

The following six CHD proteins were found in the rice genome: CHR705, CHR702, CHR703, CHR729, CHR723, and CHR744.[54] Among these proteins, five are members of the CHD3 subfamily, while CHR705 is a member of the CHD1 subfamily. In comparison to other proteins, CHR729 has been the subject of more thorough investigations. Six other allelic

https://doi.org/10.1021/acs.jafc.4c04248
J. Agric. Food Chem. 2024, 72, 19629−19643

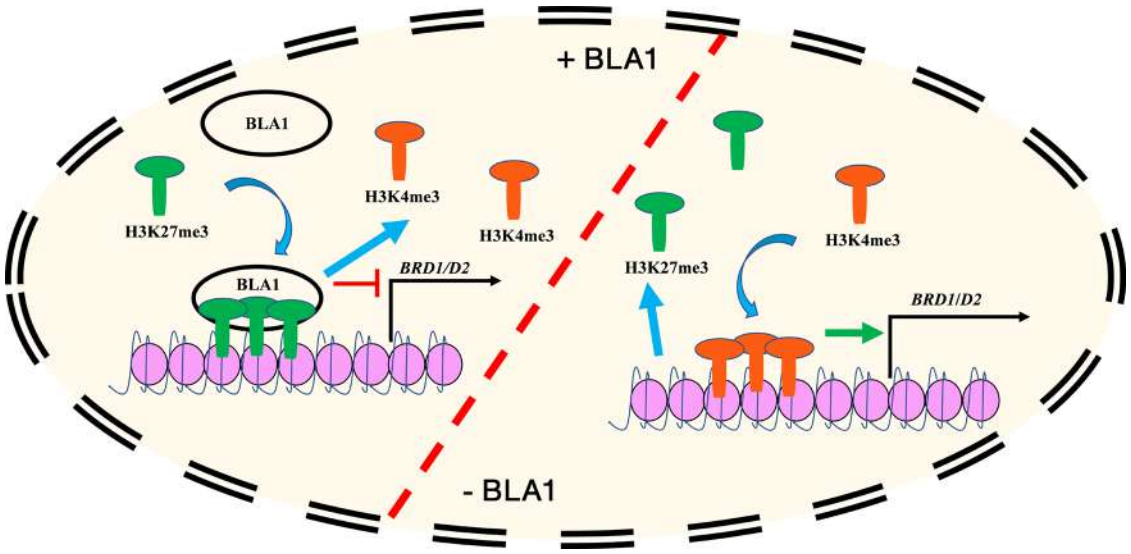

Figure 9. Possible model for the regulation of *BRD1* and *D2* transcription by BLA1.

mutants of CHR729 have been identified in earlier research, and these mutants all display consistent traits such as adaxial albino,[44] dwarfism,[33] narrow leaves, enhanced drought tolerance,[36] sluggish germination,[32] and irregular crown root development.[34] A new allelic mutant of CHR729, known as *bla1*, was identified during the screening of mutants linked to BRs. In addition to the abnormalities linked to gene mutation, it was noted that the mutant's leaf angle was noticeably greater than that of the wild-type (Figure 1). Interestingly, Wang et al. showed that the *crl6* mutant also exhibited significantly bigger flag leaf angles than the wild-type.[34] Furthermore, the mutant showed an increase in the endogenous BR content that was linked to the upregulated expression of BR synthesis genes, *BRD1* and *D2*, and the enrichment of H3K4me3 on *BRD1* and *D2* regulated by BLA1.

BRs are produced by a multienzyme biosynthesis pathway in plants. Nevertheless, little is known about how the genes encoding these enzymes are regulated, especially when it comes to epigenetic mechanisms. Evidence from this work has demonstrated that BLA1 controls the expression of *BRD1* and *D2* that negatively inhibit the production of BR. Mutant alleles of *BLA1*, including *bla1* (Figure 1), *t483* (Figure 3), and *crl6*, displayed increased leaf angles, which is a typical reaction to BR in rice.[34,55] Additionally, it was discovered that mutant lines had longer mesocotyls in darkness than the wild-type (Figures 1 and 3), a process that is highly dependent on BR.[50] The endogenous BR level measurement verified a rise in mutants, and these abnormalities may be restored by BRZ treatment (Figures 5 and S7). All of these findings imply that a loss function of BLA1 affects the BR biosynthesis pathway. Although BLA1/OsCHR4 has been shown to possess a variety of functions, our research further demonstrated these functions in plant development.

Histone modifications play a crucial role in regulating plant growth by influencing chromatin structure and transcription activity.[56] In heterochromatin sections of the plant genome, for instance, histone H3 lysine 9 monomethylation and dimethylation (H3K9me1 and H3K9me2) are associated with the maintenance of repressive states.[57] In contrast, H3K4me3 is linked to genes that are actively transcribed, and it is especially prevalent near transcriptional start sites.[58] H3K27me1 and H3K27me3 both have repressive functions,[59] and the co-occurrence of active H3K4me3 and repressive H3K27me3 marks at the same genomic locations may result in coregulation of gene transcription.[60] The evolutionarily conserved polycomb repressive complex 2 in *Arabidopsis* facilitates the deposition of H3K27me3 at different phases of plant development.[61] Research has shown that the PHD finger and trimethylated histone H3 lysine 27 interact with chromodomains of the rice CHD3 protein, CHR729, to affect several aspects of plant growth.[33] Furthermore, in agreement with earlier research,[35] our results implied that BLA1 deletion caused a global decline in the levels of H3K27me3 and H3K4me3 (Figure S10), and this may have an effect on the transcriptional regulation of BR synthesis-related genes. Our ChIP-qPCR results showed lower H3K4me3 levels for *BRD2* and decreased H3K27me3 levels for *BRD1*, *BRD2*, and *OsCPD1* (Figure 6K,L,N,O). Interestingly, several genes, such as *BRD1*, *D2*, and *OsCPD1*, showed higher amounts of H3K4me3 compared with the wild-type (Figure 6C,E,G). In agreement with the ChIP-qPCR findings, the RT-qPCR analysis confirmed the increase in the expression levels of *BRD1* and *D2* in the absence of BLA1 (Figure 6B). In addition, BLA1's binding to the promoter regions of *BRD1* and *D2* was validated using the Y1H assays (Figure 7). Moreover, in agreement with earlier research, the *d2* mutant had nonelongated mesocotyls (Figure 8).[62] However, researchers have also noted that the *brd1* mutant exhibits a phenotype that is comparable to the *d2* mutant.[17] Remarkably, unlike *BRD1* and *D2*, *BRD2* and *OsCPD1* did not show statistically significant changes between the wild-type and *bla1* mutant (Figure 6B). This discrepancy implies that other variables might be involved in the control of *BRD2* and *OsCPD1* expression. The aforementioned discoveries have greatly broadened our understanding of the CHR729 epigenetic regulatory network concerning BR production, illuminated its target genes, and improved our understanding of its function in plant growth.

To summarize, BLA1 modulated the histone methylation levels of BR synthesis genes, which is a crucial step in controlling endogenous BR synthesis in plants. BLA1 specifically suppressed the expression levels of *BRD1* and *D2*

https://doi.org/10.1021/acs.jafc.4c04248
J. Agric. Food Chem. 2024, 72, 19629−19643

by lowering the levels of H3K4me3 at their promoters. Furthermore, transcriptional downregulation caused by elevated levels of H3K27me3 at the *BRD1* promoter inhibited BR production, reducing leaf angles and shortening mesocotyls (Figure 9).

■ ASSOCIATED CONTENT

Supporting Information

The Supporting Information is available free of charge at https://pubs.acs.org/doi/10.1021/acs.jafc.4c04248.

Phenotypic characterization of the *bla1* mutant; transmission electron microscopy (TEM) of chloroplasts of the wild type (WT, first line) and *bla1* mutant (two lines below) seedlings at 40-day-old; characterization of *t483,* another mutant line of *LOC_Os07g31450*; phenotypic characterization of wild-type (WT) and complementary plants; phylogenetic tree and sequence analysis of BLA1 homologues; expression pattern of *BLA1*; phenotype of *t483* mutant rescued by treatment of BRZ; BLA1 regulates BR biosynthesis not BR signaling; BLA1 regulates expression of gene related to BR biosynthesis; accumulation of modified histone proteins; expression of two control genes; agronomic characters and photosynthetic parameters in wild-type and *bla1* mutant; and list of primers used in this study (PDF)

■ AUTHOR INFORMATION

Corresponding Authors

Limin Wu − *College of Life and Environmental Sciences, Hangzhou Normal University, Hangzhou 311121, China*; Email: lmwu2006@aliyun.com

Yanchun Yu − *College of Life and Environmental Sciences, Hangzhou Normal University, Hangzhou 311121, China*; Email: ycyu@hznu.edu.cn

Authors

Yanli Zhang − *College of Life and Environmental Sciences, Hangzhou Normal University, Hangzhou 311121, China; School of Life Sciences, Central South University, Changsha 410083 Hunan, China*; orcid.org/0000-0003-4791-7863

Guojun Dong − *State Key Laboratory for Rice Biology, China National Rice Research Institute, Hangzhou 310006 Zhejiang, China*

Ying Zhang − *College of Life and Environmental Sciences, Hangzhou Normal University, Hangzhou 311121, China*

Yaohuang Jiang − *College of Life and Environmental Sciences, Hangzhou Normal University, Hangzhou 311121, China*

Fei Chen − *College of Life and Environmental Sciences, Hangzhou Normal University, Hangzhou 311121, China*

Banpu Ruan − *College of Life and Environmental Sciences, Hangzhou Normal University, Hangzhou 311121, China*

Complete contact information is available at: https://pubs.acs.org/10.1021/acs.jafc.4c04248

Author Contributions

Y.Z. and Y.Y. designed the research. Y.Z., L.W., F.C. and B.R. performed the experiments. Ying Z., Y.J. and Y.Z. analyzed the data. Y.Y., L.W., and Y.Z. wrote the paper.

Notes

The authors declare no competing financial interest.

■ ACKNOWLEDGMENTS

We thank Dr. Longzhi Han (Chinese Academy of Agricultural Sciences) and Dr. Hong Yu (Institute of Genetics and Developmental Biology, Chinese Academy of Sciences) for kindly gifting the *t483* and *d2* mutants. We also thank Dr. Chuanzao Mao (Zhejiang University) for kindly gifting the CaMV35S::OsCHR4::GFP plasmid and the complementary lines. This work was supported by funds from the National Natural Science Foundation of China (32370328 to L.W.), "Guide Plan" of Zhejiang Province (2022R52027 to Y.Y.), and the Natural Science Foundation of Zhejiang (LY23C130001 to B.R.). We thank LetPub (www.letpub.com.cn) for its linguistic assistance during the preparation of this manuscript.

■ REFERENCES

(1) Clouse, S. D.; Sasse, J. M. BRASSINOSTEROIDS: Essential Regulators of Plant Growth and Development. *Annu Rev Plant Physiol Plant Mol Biol* **1998**, *49*, 427−451.

(2) Sun, S.; Chen, D.; Li, X.; Qiao, S.; Shi, C.; Li, C.; Shen, H.; Wang, X. Brassinosteroid signaling regulates leaf erectness in Oryza sativa via the control of a specific U-type cyclin and cell proliferation. *Dev Cell* **2015**, *34* (2), 220−228.

(3) Sakamoto, T. Phytohormones and rice crop yield: strategies and opportunities for genetic improvement. *Transgenic research* **2006**, *15* (4), 399−404.

(4) Bajguz, A.; Chmur, M.; Gruszka, D. Comprehensive Overview of the Brassinosteroid Biosynthesis Pathways: Substrates, Products, Inhibitors, and Connections. *Front Plant Sci* **2020**, *11*, 1034.

(5) Lichtenthaler, H. K. Non-mevalonate isoprenoid biosynthesis: enzymes, genes and inhibitors. *Biochemical Society transactions* **2000**, *28* (6), 785−789.

(6) Rasbery, J. M.; Shan, H.; LeClair, R. J.; Norman, M.; Matsuda, S. P.; Bartel, B. Arabidopsis thaliana squalene epoxidase 1 is essential for root and seed development. *J. Biol. Chem.* **2007**, *282* (23), 17002−17013.

(7) Zhao, B. L.; Li, J. Regulation of Brassinosteroid Biosynthesis and Inactivation. *Journal of Integrative Plant Biology* **2012**, *54* (10), 746−759.

(8) Fujioka, S.; Yokota, T. Biosynthesis and metabolism of brassinosteroids. *Annu Rev Plant Biol* **2003**, *54*, 137−164.

(9) Fujita, S.; Ohnishi, T.; Watanabe, B.; Yokota, T.; Takatsuto, S.; Fujioka, S.; Yoshida, S.; Sakata, K.; Mizutani, M. Arabidopsis CYP90B1 catalyses the early C-22 hydroxylation of C27, C28 and C29 sterols. *Plant J* **2006**, *45* (5), 765−774.

(10) Wei, Z.; Li, J. Regulation of Brassinosteroid Homeostasis in Higher Plants. *Front Plant Sci* **2020**, *11*, No. 583622.

(11) Xia, K.; Ou, X.; Tang, H.; Wang, R.; Wu, P.; Jia, Y.; Wei, X.; Xu, X.; Kang, S. H.; Kim, S. K.; et al. Rice microRNA osa-miR1848 targets the obtusifoliol 14alpha-demethylase gene OsCYP51G3 and mediates the biosynthesis of phytosterols and brassinosteroids during development and in response to stress. *New Phytol* **2015**, *208* (3), 790−802.

(12) Qin, R.; Zeng, D.; Yang, C.; Akhter, D.; Alamin, M.; Jin, X.; Shi, C. LTBSG1, a New Allele of BRD2, Regulates Panicle and Grain Development in Rice by Brassinosteroid Biosynthetic Pathway. *Genes (Basel)* **2018**, *9* (6), 292.

(13) Sakamoto, T.; Morinaka, Y.; Ohnishi, T.; Sunohara, H.; Fujioka, S.; Ueguchi-Tanaka, M.; Mizutani, M.; Sakata, K.; Takatsuto, S.; Yoshida, S.; et al. Erect leaves caused by brassinosteroid deficiency increase biomass production and grain yield in rice. *Nat. Biotechnol.* **2006**, *24* (1), 105−109.

(14) Sakamoto, T.; Ohnishi, T.; Fujioka, S.; Watanabe, B.; Mizutani, M. Rice CYP90D2 and CYP90D3 catalyze C-23 hydroxylation of brassinosteroids in vitro. *Plant Physiol Biochem* **2012**, *58*, 220−226.

(15) Sakamoto, T.; Matsuoka, M. Characterization of CONSTITUTIVE PHOTOMORPHOGENESIS AND DWARFISM homologs in rice (Oryza sativa L.). *Journal of Plant Growth Regulation* **2006**, *25* (3), 245−251.

(16) Tanabe, S.; Ashikari, M.; Fujioka, S.; Takatsuto, S.; Yoshida, S.; Yano, M.; Yoshimura, A.; Kitano, H.; Matsuoka, M.; Fujisawa, Y.; et al. A novel cytochrome P450 is implicated in brassinosteroid biosynthesis via the characterization of a rice dwarf mutant, dwarf11, with reduced seed length. *Plant Cell* **2005**, *17* (3), 776−790.
(17) Hong, Z.; Ueguchi-Tanaka, M.; Shimizu-Sato, S.; Inukai, Y.; Fujioka, S.; Shimada, Y.; Takatsuto, S.; Agetsuma, M.; Yoshida, S.; Watanabe, Y.; et al. Loss-of-function of a rice brassinosteroid biosynthetic enzyme, C-6 oxidase, prevents the organized arrangement and polar elongation of cells in the leaves and stem. *Plant J* **2002**, *32* (4), 495−508.
(18) Clouse, S. D.; Langford, M.; McMorris, T. C. A brassinosteroid-insensitive mutant in Arabidopsis thaliana exhibits multiple defects in growth and development. *Plant Physiol* **1996**, *111* (3), 671−678.
(19) Wang, L.; Wang, Z.; Xu, Y. Y.; Joo, S. H.; Kim, S. K.; Xue, Z.; Xu, Z. H.; Wang, Z. Y.; Chong, K. OsGSR1 is involved in crosstalk between gibberellins and brassinosteroids in rice. *Plant Journal* **2009**, *57* (3), 498−510.
(20) Gan, L.; Wu, H.; Wu, D.; Zhang, Z.; Guo, Z.; Yang, N.; Xia, K.; Zhou, X.; Oh, K.; Matsuoka, M.; et al. Methyl jasmonate inhibits lamina joint inclination by repressing brassinosteroid biosynthesis and signaling in rice. *Plant Sci* **2015**, *241*, 238−245.
(21) Li, Q. F.; Lu, J.; Zhou, Y.; Wu, F.; Tong, H. N.; Wang, J. D.; Yu, J. W.; Zhang, C. Q.; Fan, X. L.; Liu, Q. Q. Abscisic Acid Represses Rice Lamina Joint Inclination by Antagonizing Brassinosteroid Biosynthesis and Signaling. *Int J Mol Sci* **2019**, *20* (19), 4908.
(22) Asahina, M.; Tamaki, Y.; Sakamoto, T.; Shibata, K.; Nomura, T.; Yokota, T. Blue light-promoted rice leaf bending and unrolling are due to up-regulated brassinosteroid biosynthesis genes accompanied by accumulation of castasterone. *Phytochemistry* **2014**, *104*, 21−29.
(23) Sui, P. F.; Jin, J.; Ye, S.; Mu, C.; Gao, J.; Feng, H. Y.; Shen, W. H.; Yu, Y.; Dong, A. W. H3K36 methylation is critical for brassinosteroid-regulated plant growth and development in rice. *Plant Journal* **2012**, *70* (2), 340−347.
(24) Zhang, X.; Sun, J.; Cao, X.; Song, X. Epigenetic Mutation of RAV6 Affects Leaf Angle and Seed Size in Rice. *Plant Physiol* **2015**, *169* (3), 2118−2128.
(25) Shimada, A.; Ueguchi-Tanaka, M.; Sakamoto, T.; Fujioka, S.; Takatsuto, S.; Yoshida, S.; Sazuka, T.; Ashikari, M.; Matsuoka, M. The rice SPINDLY gene functions as a negative regulator of gibberellin signaling by controlling the suppressive function of the DELLA protein, SLR1, and modulating brassinosteroid synthesis. *Plant Journal* **2006**, *48* (3), 390−402.
(26) Flaus, A.; Martin, D. M.; Barton, G. J.; Owen-Hughes, T. Identification of multiple distinct Snf2 subfamilies with conserved structural motifs. *Nucleic Acids Res.* **2006**, *34* (10), 2887−2905.
(27) Lu, Y.; Tan, F.; Zhao, Y.; Zhou, S.; Chen, X.; Hu, Y.; Zhou, D. X. A Chromodomain-Helicase-DNA-Binding Factor Functions in Chromatin Modification and Gene Regulation. *Plant Physiol* **2020**, *183* (3), 1035−1046.
(28) Shen, Y.; Devic, M.; Lepiniec, L.; Zhou, D. X. Chromodomain, Helicase and DNA-binding CHD1 protein, CHR5, are involved in establishing active chromatin state of seed maturation genes. *Plant Biotechnol J* **2015**, *13* (6), 811−820.
(29) Zhang, H.; Rider, S. D., Jr.; Henderson, J. T.; Fountain, M.; Chuang, K.; Kandachar, V.; Simons, A.; Edenberg, H. J.; Romero-Severson, J.; Muir, W. M.; et al. The CHD3 remodeler PICKLE promotes trimethylation of histone H3 lysine 27. *J. Biol. Chem.* **2008**, *283* (33), 22637−22648.
(30) Carter, B.; Bishop, B.; Ho, K. K.; Huang, R.; Jia, W.; Zhang, H.; Pascuzzi, P. E.; Deal, R. B.; Ogas, J. The Chromatin Remodelers PKL and PIE1 Act in an Epigenetic Pathway That Determines H3K27me3 Homeostasis in Arabidopsis. *Plant Cell* **2018**, *30* (6), 1337−1352.
(31) Sang, Q.; Pajoro, A.; Sun, H.; Song, B.; Yang, X.; Stolze, S. C.; Andres, F.; Schneeberger, K.; Nakagami, H.; Coupland, G. Mutagenesis of a Quintuple Mutant Impaired in Environmental Responses Reveals Roles for CHROMATIN REMODELING4 in the Arabidopsis Floral Transition. *Plant Cell* **2020**, *32* (5), 1479−1500.
(32) Ma, X. D.; Ma, J.; Zhai, H. H.; Xin, P. Y.; Chu, J. F.; Qiao, Y. L.; Han, L. Z. CHR729 Is a CHD3 Protein That Controls Seedling Development in Rice. *Plos One* **2015**, *10* (9), No. e0138934.
(33) Hu, Y.; Liu, D.; Zhong, X.; Zhang, C.; Zhang, Q.; Zhou, D. X. CHD3 protein recognizes and regulates methylated histone H3 lysines 4 and 27 over a subset of targets in the rice genome. *Proc Natl Acad Sci U S A* **2012**, *109* (15), 5773−5778.
(34) Wang, Y.; Wang, D.; Gan, T.; Liu, L.; Long, W.; Wang, Y.; Niu, M.; Li, X.; Zheng, M.; Jiang, L.; et al. CRL6, a member of the CHD protein family, is required for crown root development in rice. *Plant Physiol Biochem* **2016**, *105*, 185−194.
(35) Cho, S. H.; Lee, C. H.; Gi, E.; Yim, Y.; Koh, H. J.; Kang, K.; Paek, N. C. The Rice Rolled Fine Striped (RFS) CHD3/Mi-2 Chromatin Remodeling Factor Epigenetically Regulates Genes Involved in Oxidative Stress Responses During Leaf Development. *Front Plant Sci* **2018**, *9*, 364.
(36) Guo, T.; Wang, D.; Fang, J.; Zhao, J.; Yuan, S.; Xiao, L.; Li, X. Mutations in the Rice OsCHR4 Gene, Encoding a CHD3 Family Chromatin Remodeler, Induce Narrow and Rolled Leaves with Increased Cuticular Wax. *Int J Mol Sci* **2019**, *20* (10), 2567.
(37) Chen, F.; Dong, G.; Wang, F.; Shi, Y.; Zhu, J.; Zhang, Y.; Ruan, B.; Wu, Y.; Feng, X.; Zhao, C.; et al. A beta-ketoacyl carrier protein reductase confers heat tolerance via the regulation of fatty acid biosynthesis and stress signaling in rice. *New Phytol* **2021**, *232* (2), 655−672.
(38) Watanabe, H.; Takahashi, K.; Saigusa, M. Morphological and anatomical effects of abscisic acid (ABA) and fluridone (FLU) on the growth of rice mesocotyls. *Plant Growth Regul* **2001**, *34* (3), 273−275.
(39) Lv, Y. S.; Shao, G. N.; Jiao, G. A.; Sheng, Z. H.; Xie, L. H.; Hu, S. K.; Tang, S. Q.; Wei, X. J.; Hu, P. S. Targeted mutagenesis of POLYAMINE OXIDASE 5 that negatively regulates mesocotyl elongation enables the generation of direct-seeding rice with improved grain yield. *Molecular Plant* **2021**, *14* (2), 344−351.
(40) Chen, F.; Dong, G.; Wu, L.; Wang, F.; Yang, X.; Ma, X.; Wang, H.; Wu, J.; Zhang, Y.; Wang, H.; et al. A Nucleus-Encoded Chloroplast Protein YL1 Is Involved in Chloroplast Development and Efficient Biogenesis of Chloroplast ATP Synthase in Rice. *Sci Rep* **2016**, *6*, 32295.
(41) Saitou, N.; Nei, M. The neighbor-joining method: a new method for reconstructing phylogenetic trees. *Mol. Biol. Evol.* **1987**, *4* (4), 406−425.
(42) Felsenstein, J. Confidence Limits on Phylogenies: An Approach Using the Bootstrap. *Evolution; international journal of organic evolution* **1985**, *39* (4), 783−791.
(43) Tamura, K.; Peterson, D.; Peterson, N.; Stecher, G.; Nei, M.; Kumar, S. MEGA5: molecular evolutionary genetics analysis using maximum likelihood, evolutionary distance, and maximum parsimony methods. *Mol. Biol. Evol.* **2011**, *28* (10), 2731−2739.
(44) Zhao, C.; Xu, J.; Chen, Y.; Mao, C.; Zhang, S.; Bai, Y.; Jiang, D.; Wu, P. Molecular cloning and characterization of OsCHR4, a rice chromatin-remodeling factor required for early chloroplast development in adaxial mesophyll. *Planta* **2012**, *236* (4), 1165−1176.
(45) Favery, B.; Chelysheva, L. A.; Lebris, M.; Jammes, F.; Marmagne, A.; De Almeida-Engler, J.; Lecomte, P.; Vaury, C.; Arkowitz, R. A.; Abad, P. Arabidopsis formin AtFH6 is a plasma membrane-associated protein upregulated in giant cells induced by parasitic nematodes. *Plant Cell* **2004**, *16* (9), 2529−2540.
(46) Liu, J. M.; Park, S. J.; Huang, J.; Lee, E. J.; Xuan, Y. H.; Je, B. I.; Kumar, V.; Priatama, R. A.; Vimal, R. K.; Kim, S. H. Loose Plant Architecture1 (LPA1) determines lamina joint bending by suppressing auxin signalling that interacts with C-22-hydroxylated and 6-deoxo brassinosteroids in rice. *J. Exp. Botany* **2016**, *67* (6), 1883−1895.
(47) Han, Y.; Chen, Z.; Lv, S.; Ning, K.; Ji, X.; Liu, X.; Wang, Q.; Liu, R.; Fan, S.; Zhang, X. MADS-Box Genes and Gibberellins Regulate Bolting in Lettuce (Lactuca sativa L.). *Front Plant Sci* **2016**, *7*, 1889.

(48) Guo, L.; Yu, Y.; Law, J. A.; Zhang, X. SET DOMAIN GROUP2 is the major histone H3 lysine [corrected] 4 trimethyltransferase in Arabidopsis. *Proc Natl Acad Sci U S A* **2010**, *107* (43), 18557−18562.
(49) Wang, Z. Y.; Nakano, T.; Gendron, J.; He, J.; Chen, M.; Vafeados, D.; Yang, Y.; Fujioka, S.; Yoshida, S.; Asami, T.; et al. Nuclear-localized BZR1 mediates brassinosteroid-induced growth and feedback suppression of brassinosteroid biosynthesis. *Dev Cell* **2002**, *2* (4), 505−513.
(50) Yamamuro, C.; Ihara, Y.; Wu, X.; Noguchi, T.; Fujioka, S.; Takatsuto, S.; Ashikari, M.; Kitano, H.; Matsuoka, M. Loss of function of a rice brassinosteroid insensitive1 homolog prevents internode elongation and bending of the lamina joint. *Plant Cell* **2000**, *12* (9), 1591−1606.
(51) Tanaka, A.; Nakagawa, H.; Tomita, C.; Shimatani, Z.; Ohtake, M.; Nomura, T.; Jiang, C. J.; Dubouzet, J. G.; Kikuchi, S.; Sekimoto, H.; et al. BRASSINOSTEROID UPREGULATED1, encoding a helix-loop-helix protein, is a novel gene involved in brassinosteroid signaling and controls bending of the lamina joint in rice. *Plant Physiol* **2009**, *151* (2), 669−680.
(52) Lippman, Z.; Gendrel, A. V.; Black, M.; Vaughn, M. W.; Dedhia, N.; McCombie, W. R.; Lavine, K.; Mittal, V.; May, B.; Kasschau, K. D. Role of transposable elements in heterochromatin and epigenetic control. *Nature* **2004**, *430* (6998), 471−476.
(53) Hu, Y.; Lai, Y.; Zhu, D. Transcription regulation by CHD proteins to control plant development. *Front Plant Sci* **2014**, *5*, 223.
(54) Hu, Y. F.; Zhu, N.; Wang, X. M.; Yi, Q. P.; Zhu, D. Y.; Lai, Y.; Zhao, Y. Analysis of rice Snf2 family proteins and their potential roles in epigenetic regulation. *Plant Physiol Bioch* **2013**, *70*, 33−42.
(55) Wada, K.; Marumo, S.; Ikekawa, N.; Morisaki, M.; Mori, K. Brassinolide and Homobrassinolide Promotion of Lamina Inclination of Rice Seedlings. *Plant Cell Physiol.* **1981**, *22* (2), 323−325.
(56) Zhao, T.; Zhan, Z. P.; Jiang, D. H. Histone modifications and their regulatory roles in plant development and environmental memory. *Journal of Genetics and Genomics* **2019**, *46* (10), 467−476.
(57) Bernatavichute, Y. V.; Zhang, X.; Cokus, S.; Pellegrini, M.; Jacobsen, S. E. Genome-wide association of histone H3 lysine nine methylation with CHG DNA methylation in Arabidopsis thaliana. *PLoS One* **2008**, *3* (9), No. e3156.
(58) Li, X. Y.; Wang, X. F.; He, K.; Ma, Y. Q.; Su, N.; He, H.; Stolc, V.; Tongprasit, W.; Jin, W. W.; Jiang, J. M.; et al. High-resolution mapping of epigenetic modifications of the rice genome uncovers interplay between DNA methylation, histone methylation, and gene expression. *Plant Cell* **2008**, *20* (2), 259−276.
(59) Zhang, X.; Clarenz, O.; Cokus, S.; Bernatavichute, Y. V.; Pellegrini, M.; Goodrich, J.; Jacobsen, S. E. Whole-genome analysis of histone H3 lysine 27 trimethylation in Arabidopsis. *PLoS biology* **2007**, *5* (5), No. e129.
(60) Jiang, D.; Wang, Y.; Wang, Y.; He, Y. Repression of FLOWERING LOCUS C and FLOWERING LOCUS T by the Arabidopsis Polycomb repressive complex 2 components. *PLoS One* **2008**, *3* (10), No. e3404.
(61) Mozgova, I.; Hennig, L. The polycomb group protein regulatory network. *Annu Rev Plant Biol* **2015**, *66*, 269−296.
(62) Hong, Z.; Ueguchi-Tanaka, M.; Umemura, K.; Uozu, S.; Fujioka, S.; Takatsuto, S.; Yoshida, S.; Ashikari, M.; Kitano, H.; Matsuoka, M. A rice brassinosteroid-deficient mutant, ebisu dwarf (d2), is caused by a loss of function of a new member of cytochrome P450. *Plant Cell* **2003**, *15* (12), 2900−2910.

https://doi.org/10.1021/acs.jafc.4c04248
J. Agric. Food Chem. 2024, 72, 19629−19643